Resolution Enhancement in Harmonic Analysis by Compressive Sensing

M. Bertocco*, G. Frigo*, C. Narduzzi*, F. Tramarin†
* University of Padua, Department of Information Engineering – DEI
via G. Gradenigo 6/b, I–35131 Padova, Italy – e-mail: {mat, frigogug, narduzzi}@dei.unipd.it
† National Research Council (CNR) of Italy, IEIIT – Padova,
via G. Gradenigo 6/b, I–35131 Padova, Italy – e-mail: tramarin@dei.unipd.it

***Abstract*—Measurement in power systems and, particularly, in smart grids and smart microgrids is often concerned with harmonic analysis of voltage and current waveforms, which can be obtained by Fourier-based algorithms (e.g., phasor measurements, power quality analysis). Any such measurement algorithm is characterized by a fundamental time-frequency resolution tradeoff that relates the sampling frequency and the signal acquisition time. These well-known conditions determine basic limits of measuring equipment, for instance, when transient response times are considered. Phasor measurement reporting latency is also affected since, for any DFT-based algorithm, this time cannot be shorter than half the observation interval. This paper presents the application of an algorithm, based on the principles of compressive sensing (CS), that enhances frequency resolution by jointly processing multiple sets of DFT coefficients, computed from time-shifted acquisitions of the same waveform. By suitably merging such information, the CS algorithm can achieve an order-of-magnitude resolution improvement without significantly extending the total observation interval, since successive acquisitions can have a very large overlap. For harmonic analysis in power systems, this means accurate results can be obtained using shorter observation intervals, which allow to effectively track changes and reduce the effect of transients on measurements.**

Keywords*—harmonic analysis, power system measurement, compressive sensing.

I. Introduction

Measurement in power systems and, particularly, in smart grids and smart microgrids is often concerned with harmonic analysis of voltage and current waveforms. Phasor measurement units (PMUs) carry out time-synchronized measurements of phasors at the fundamental line frequency. These are often obtained by Fourier-based algorithms, although the basic estimation model provided in [1] relies on a digital quadrature demodulator. Power quality analyzers (PQAs) employ the Fourier transform to determine the harmonic content of waveforms at selected points in a network.

Any such measurement algorithm is characterized by a fundamental time-frequency resolution tradeoff, that follows directly from limitations related to the sampling frequency and the signal acquisition time. Given that the sampling frequency f_s is determined according to the requirements of Shannon's theorem and any acquisition system will be able to acquire at most N samples, the granularity of measurements on the frequency axis equals the reciprocal of the observation interval, i.e., f_s/N. Since in discrete Fourier transform (DFT) algorithms granularity is directly related to frequency resolution, any resolution improvement can only be paid for by an increase in measurement time. It is also clear that, to resolve harmonics of the power-line frequency, the minimum observation interval would have to be at least one waveform period and, in practice, rather longer.

These well-known conditions determine basic limits of measuring equipment, particularly when transient responses are considered. For instance, [1] allows PMU response times well in excess of one period of the fundamental frequency for specified step changes, either in magnitude or phase of the measured waveform. Reporting latency is also affected since, for any DFT-based algorithm, it cannot be shorter than a half of the observation interval.

Resolution and accuracy in harmonic analysis are limited by the effects of spectral leakage, which causes interference among neighboring frequency components of the analyzed waveform. The extent of these effects depends on the amplitudes and frequency separation of the involved components, as well as on their *instantaneous phases*. In fact, any periodic signal can be expressed in time as a sum of complex exponential terms, whose corresponding individual complex DFT coefficients are combined by vector summation to produce the waveform DFT. It can be easily realized, by comparing the frequency spectra of a generic waveform computed from sample acquisitions taken at different times, that interference patterns differ, even though the waveform composition has not changed. This is a consequence of the different instantaneous phase values taken up by each component at different times. It becomes almost natural, then, to investigate whether such additional knowledge can be exploited to enhance spectral estimation of waveforms.

This paper presents the application of an algorithm, based on the principles of compressive sensing (CS), that enhances frequency resolution by jointly processing multiple sets of DFT coefficients computed from time-shifted acquisitions of the same waveform. By suitably merging such information, the CS algorithm can achieve an order-of-magnitude improvement in frequency granularity without significantly extending the total observation interval, since successive acquisitions can have a very large overlap [2]. While application of the CS algorithm does not eliminate spectral leakage, by reducing granularity on the frequency axis it increases, in normalised terms, the frequency separation between adjacent components. This virtually eliminates long-range frequency interference

effects, leaving only scalloping loss to be dealt with. Of course, computational complexity of the algorithm is higher, but still within manageable limits for the processing capabilities of current equipment. The end result is that a similar order-of-magnitude improvement can be achieved in frequency resolution, with a bare 5% increase in measurement time.

For harmonic analysis in power systems, this means accurate results can be obtained using shorter observation intervals, which allow to effectively track changes and reduce the effect of transients on measurements. More detailed results will be presented in the full paper.

II. Harmonic Analysis Summary

A harmonic waveform can be expressed by the sum of a number of complex exponential components (with suitable symmetries):

$$s(t) = \sum_h \left[\frac{A_h}{2} e^{+j(\phi_h + 2\pi h f_0 t)} + \frac{A_h}{2} e^{-j(\phi_h + 2\pi h f_0 t)} \right], \qquad (1)$$

where f_0 is the fundamental frequency. The DFT algorithm processes a set of N waveform samples, taken at the sampling frequency f_s, and provides the corresponding N DFT coefficients, that can be expressed by the equation:

$$S\left(\frac{k}{N}\right) = \sum_{h \in S_H} \frac{A_h}{2} e^{j\phi_h} D_N\left(\frac{k}{N} - \lambda_h\right) e^{-j2\pi\left(\frac{k}{N} - \lambda_h\right) n_0}, \quad 0 \le k < N, \qquad (2)$$

where $\lambda_h = h \cdot (f_0/f_s)$ is the normalized frequency of the h-th harmonic component, n_0 is the index of the start sample in the acquired sequence and $D_N(\cdot)$ is the Dirichlet kernel:

$$D_N(\lambda) = \frac{\sin \pi N \lambda}{N \sin \pi \lambda} e^{-j\pi(N-1)\lambda}. \qquad (3)$$

DFT coefficients in (2) are given at discrete normalized frequency values $\lambda = k/N$, that is, for integer multiples of the frequency granularity f_s/N, or $1/N$ in normalized terms [3].

Symmetries characterizing any waveform defined as a real function imply that a component at normalized frequency λ_h has a corresponding image, satisfying the usual Hermitian conditions on amplitude and phase, whose normalized frequency in (2) appears as $1 - \lambda_h$. The summation condition $h \in S_H$ is intended to reflect this, meaning that S_H is the set that includes all contributing complex exponential terms.

It is well-known that, because of the shape of the Dirichlet kernel, significant frequency interference between adjacent frequency components can already occur at normalized distances as large as ten times the granularity so that, to avoid inaccuracies, observation intervals longer than $10/f_0$ would be required. Of course, the weighting of time-domain samples by a suitable window reduces long-range interference effects and, coupled with frequency interpolation, can provide better harmonic analysis accuracy with shorter observation intervals. The need to allow for window mainlobe widths still means that, in general, observation intervals between two and four waveform cycles need to be considered for phasor measurements [4], [5].

III. Sparsity and Compressive Sensing

The CS algorithm employed in this work considers a small set of M measurement vectors, each composed of the DFT coefficients calculated from a different record of N waveform samples. The index of the first sample in each record is assumed to be known, which is straighforward since, without loss of generality, one may set this to zero for the first acquisition, and simply record the index difference at the start of subsequent records. With this convention, the start index will be indicated by n_m, with $n_0 = 0$. Given a sample record with start index n_m, it is useful to rewrite its DFT coefficients in the slightly modified form:

$$S_m\left(\frac{k}{N}\right) = \sum_{h \in S_H} \left[\frac{A_h}{2} e^{j(\phi_h - 2\pi\lambda_h n_m)} \cdot D_N\left(\frac{k}{N} - \lambda_h\right) \cdot e^{-j2\pi \frac{k}{N} n_m} \right], \qquad (4)$$

that evidences an exponential term (the last term within brackets in (4)) which is independent of the normalized frequency. This term can be set to zero by the simple expedient of conventionally assigning the index 0 to the first element of a record whenever a DFT is computed, which is actually what happens in practice.

The subscript $0 \le m < M$ allows to refer unambiguously both to a record and to its corresponding DFT vector. The latter will be represented in the following as a column vector: $\mathbf{s}_m = [S_m(0), S_m(\frac{1}{N}), \ldots, S_m(\frac{k}{N}), \ldots, S_m(\frac{N-1}{N})]^T$. Measurement information can then be arranged into a $N \times M$ matrix, in the form: $\mathbf{S} = [\mathbf{s}_0\ \mathbf{s}_1 \ldots\ \mathbf{s}_{M-1}]$. From the discussion above, it follows that a generic element of this matrix is defined by the expression:

$$s_{k,m} = \sum_{h \in S_H} \frac{A_h}{2} e^{j(\phi_h - 2\pi\lambda_h n_m)} D_N\left(\frac{k}{N} - \lambda_h\right) \qquad (5)$$

where n_m is known. This is a key point in the method under discussion. While NM different elements are needed to fill the matrix $\mathbf{S}$, this does not imply that NM entirely different time-domain samples are required. In fact, shifting the start of the time-domain record, even by few samples, introduces different phase rotations in DFT contributions at different frequencies. The consequent variety in the resulting vector sums in (5) is enough to ensure that columns of $\mathbf{S}$ are linearly independent, even when *heavily overlapping* time-domain sample records are employed in DFT computations.

The second important element in the problem is that, since the observed waveform is always the same, all column vectors $\mathbf{s}_m$ are generated from a *common* set of frequencies λ_h, with $h \in S_H$. Unfortunately vector elements depend continuously on the unknown frequencies, however one may define a new frequency grid with normalized granularity $1/N'$, $N' > N$ and assume, to a first approximation, that waveform frequencies do lie exactly on this denser grid.

Indicating by l_h the integer that yields:

$$\lambda_h = \frac{l_h}{N'}, \qquad (6)$$

equation (5) can be rewritten as:

$$s_{k,m} = \sum_{l \in S_L} \frac{A_l}{2} e^{j(\phi_l - 2\pi \frac{l}{N'} n_m)} D_N\left(\frac{k}{N} - \frac{l}{N'}\right) \qquad (7)$$

where: $S_L \subset \{0,\ 1,\ \ldots,\ N'-1\}$ is the set of integer values of l that correspond to some waveform component and is called the *support* of $s(t)$.

As component frequencies are not known, the algorithm has to consider that any value of the index l, with $0 \le l < N'$, may be contained in the support. The only *a priori* constraint is that, given the assumptions above, the number of elements in S_L, indicated by $|S_L|$, must be small compared to N', i.e., the support is *sparse*: $|S_L| \ll N'$.

Introducing the matrix $\mathbf{D}$, whose elements are defined by: $d_{k,l} = D_N\left(\frac{k}{N} - \frac{l}{N'}\right)$ and the matrix $\mathbf{W} = \left[\mathbf{w}_{N'}^{n_0}\ \mathbf{w}_{N'}^{n_1}\ \mathbf{w}_{N'}^{n_{M-1}}\right]$, where elements of the generic vector $\mathbf{w}_{N'}^{n_m}$ are: $\mathbf{w}_{N'}^{n_m}[l] = e^{j2\pi\frac{l}{N'}n_m}$, $0 \le l < N'$, it follows that $\mathbf{S}$ can be factorized as:

$$\mathbf{S} = \mathbf{DAW} = \mathbf{D}\begin{bmatrix} \frac{A_0}{2}e^{j\phi_0} & \ldots & 0 \\ 0 & \frac{A_1}{2}e^{j\phi_1} & 0 \\ \vdots & \ddots & \vdots \\ 0 & \ldots & \frac{A_{N'-1}}{2}e^{j\phi_{N'-1}} \end{bmatrix}\mathbf{W}. \quad (8)$$

where only a few elements on the main diagonal of $\mathbf{A}$ are non-zero, because of sparsity.

It can be noticed that the $N \times N'$ matrix $\mathbf{D}$ in (8) represents the effect of spectral leakage, through values of the Dirichlet kernel computed on a suitable two-dimensional grid. Non-zero rows in the $N' \times M$ matrix product $\mathbf{X} = \mathbf{AW}$ correspond to elements whose row index belong to the support set S_L. In CS parlance, the columns of $\mathbf{X}$ are a set of jointly sparse vectors with common support S_L.

Support recovery is the first step of the CS algorithm and has the purpose of determining the set S_L, which defines the frequency locations of the waveform components. For this purpose the procedure given in [6] is followed. Once S_L is known, the next step involves the construction of a restricted matrix $\mathbf{D}_S$, obtained by deleting the columns of $\mathbf{D}$ whose index l is not in S_L. This turns (8) into an overdetermined matrix equation, that can be solved by computing the pseudo-inverse:

$$\hat{\mathbf{X}}_S = \left(\mathbf{D}_S^H\mathbf{D}_S\right)^{-1}\mathbf{D}_S^H\mathbf{S} \quad (9)$$

which yields the non-zero rows of $\mathbf{X}$. Finally, the amplitudes and phases of non-zero components in $\mathbf{A}$ are reconstructed. Some details of this procedure are given in [2].

IV. Discussion and Results

Simulation analysis shows that, when no noise affects the signal and normalized component frequencies are exactly given as l_h/N', the algorithm can reconstruct component amplitudes and phases exactly (to within machine error). Of course, the two conditions point to an ideal situation, which is hardly found in practice.

As far as the determination of frequency is concerned, the CS algorithm provides improved frequency granularity, but does not allow frequency resolution to become infinitely small. Nevertheless, assuming $N' = P \cdot N$ is equivalent to the application of an integer *interpolation factor* to the frequency grid, which is made denser by the factor P.

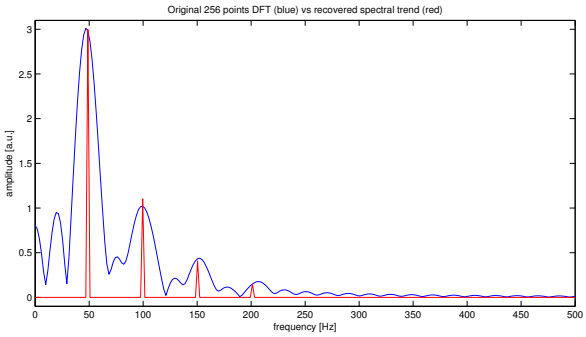

Fig. 1. comparison between magnitude estimates of a 4-harmonic periodic waveform obtained with a single 256-point DFT and withn the CS-based algorithm.

Support recovery is the critical part of the algorithm, as its task is to identify waveform components. Its function is the equivalent, on the equivalent denser frequency grid, of peak search in traditional DFT-based spectral analysis. In a similar fashion, a non-linear threshold effect can be noticed, whereby support detection begins to fail as the signal-to-noise ratio (SNR) drops below 20 dB [2]. This can be considered an acceptable performance limitation in power system measurement, with the possible exception of noise temporarily induced by transient phenomena such as lightning strikes or the opening of circuit breakers.

In the example shown in Fig. 1, a periodic waveform composed of four harmonic terms is considered. The CS algorithm processes $M = 64$ sets of DFT coefficients obtained from data records containing 256 samples each, acquired with a sampling frequency $f_s = 5000$ Hz. The frequencies of the four terms fall exactly on points of the equivalent denser grid, which are correctly identified by the CS support recovery procedure. The corrsponding amplitude estimates correspond to sharp peaks in the figure.

The spectrum magnitude computed from a single 256-point DFT, zero-padded to lie on the same dense grid, is also shown for comparison. It can be seen that the latter is significantly affected by interference among the waveform components, to the extent that the positions of its peaks have been slightly altered. It should be remarked that, as the actual positions of coefficients in a 256-point DFT can only be referred to the original frequency granularity, they would not even correspond to those peaks, hence DFT-based magnitude estimates could be much worse (in practice, a weighted interpolated DFT algorithm could be employed to recover some accuracy, as far as possible).

A preliminary assessment of measurement uncertainty can be obtained by simulation analysis. Results reported in Table I refer to the amplitude estimates of harmonic components, for the same waveform whose spectrum is shown in Fig. 1. Additive noise giving a 40 dB SNR is assumed, which can be representative of practical situations where a low-resolution (8 bit) analog-to-digital converter is employed to acquire the waveform. Of course, from the theoretical viewpoint the matrix $\mathbf{S}$ should then be replaced in (9) by the measurement matrix:

$$\mathbf{Y} = \mathbf{S} + \mathbf{N}, \quad (10)$$

TABLE I. AMPLITUDE ESTIMATION FOR CS-BASED ESTIMATION OF A WAVEFORM WITH FOUR HARMONIC COMPONENTS – SNR = 40 DB

harmonic no.	**1**	**2**	**3**	**4**
reference amplitude	6	2.21	0.812	0.299
mean deviation (%)	-3.4×10^{-5}	-1.3×10^{-4}	-1.3×10^{-4}	-2.3×10^{-4}
std. deviation (%)	2.6×10^{-4}	5.6×10^{-4}	1.9×10^{-3}	5.1×10^{-3}

where $\mathbf{N}$ accounts for the noise components. Because of the way DFT coefficients are computed, it is known that each column of this matrix is a random vector having independent, identically distributed zero-mean Gaussian complex elements.

Table I summarizes results from a set of 100 simulation runs for the proposed CS algorithm. It can be seen that estimation bias is negligible, since the relative mean deviation from the corresponding reference amplitude is almost one order of magnitude smaller than the relative standard deviation, for all four harmonic components. Considering a coverage factor equal to 3, uncertainty for the phasor magnitude of the fundamental component results to be better than 0.1%.

Similarly good results were found for phase estimates, where estimation uncertainty ranges from 0.03 degrees for the fundamental component to 0.4 degrees for the fourth harmonic.

It has to be mentioned that, for the smaller components, noise may sometimes affect the outcome of the support recovery procedure. In fact in a single case, out of 100 simulations, the frequency of the third harmonic component was not estimated correctly. Consequently, results reported for this component do not include the outcome of the simulation run where support recovery partly failed.

An important contribution of the algorithm is that frequency granularity improvement by about one order of magnitude is achievable without significantly increasing measurement time. The condition $M \geq |S_L|$ is clearly necessary to obtain the solution (9) but, as already noted, this does not imply non-overlapping data records. Thus, assuming the average delay between two consecutive acquisitions is Δn, the total acquisition time is just $(N + M \cdot \Delta n)/f_s$ and overlaps larger than 90% have been found feasible. It should also be remarked, with reference to results presented in Table I, that repetition of the simulation test with the same SNR value, but using $M = 8$ instead of $M = 64$ for the CS algorithm, yielded an increase in estimation variance by approximately an order of magnitude, which suggests variance scales as $1/M$.

Analysis of the preliminary results presented above thus points to the possibility of using comparatively few sets of DFT coefficients, obtained from broadly overlapping data acquisitions, to achieve the desired target accuracies. The value of M, of course, depends on the assumed number of waveform harmonics. In the four-harmonics example discussed above the smallest value giving sufficiently accurate results is $M = 8$. A very high overlap between consecutive data records has been tested and found feasible, yielding $\Delta_n = 3$ so that, with the assumed parameters, the actual acquisition time can be made as low as $(256 + 8 \times 3)/5000 = 56$ ms.

It can also be noticed that the data acquisition parameters considered so far were chosen to allow comparison with a simple DFT algorithm. However, the CS algorithm enables parameter choices resulting in even shorter observation intervals, which could not be considered for a normal DFT-based algorithm. To put this achievement in a power measurement context, this means DFT-based phasor measurement or power quality analysis could be carried out with $f_s = 4000$ Hz and $N = 128$ (a 32 ms observation interval) and, by combining a set of M acquisitions through the CS algorithm, a resolution equivalent to a 320 ms observation interval can be achieved.

Of course, computational complexity of the CS algorithm is higher than a simple DFT, but still within manageable limits for the processing capabilities of current equipment. In particular, computation of DFT coefficients by an FFT algorithm is a highly parallelizable task that can be implemented efficiently on a field-programmable gate array (FPGA) architecture. This allows to quickly build up the measurement matrix $\mathbf{Y}$, while leaving to a main processor in the measuring equipment the more complex CS algorithm.

An issue that remains to be discussed concerns the actual location of the measured waveform components on the frequency axis. If the actual normalized frequency of a waveform component cannot be expressed exactly as l_h/N', the corresponding amplitude estimate can be significantly smaller than the reference value. This effect appears to be strictly related to the Dirichlet kernel scalloping loss and it should be possible to deal with it by some simple interpolation approach [3]. A more detailed discussion of this point will be presented in the final form of this paper.

REFERENCES

[1] IEEE Std C37.118.1-2011, "IEEE Standard for Synchrophasor Measurements for Power Systems", IEEE, New York, USA, 2011.

[2] M. Bertocco, G. Frigo, C. Narduzzi, "On compressed sensing and super-resolution in DFT-based spectral analysis", Proceedings 19th IMEKO TC-4 Symposium and 17th IWADC Workshop *Advances in Instrumentation and Sensors Interoperability*, July 18-19, 2013, Barcelona, Spain.

[3] V. H. Jain, W. L. Collins and D. C. Davis, "High accuracy analog measurements via interpolated FFT", *IEEE Trans. Instrum. Meas.*, vol. 28, no. 1, pp. 113-122, Jan. 1979.

[4] M. Bertocco, C. Narduzzi, F. Tramarin, "Characterization of microgrid smart metering: phasor estimation under impaired conditions", Proc. 2013 Int. Instrum. Meas. Technol. Conf., I2MTC 2013, May 6-9, 2013, Minneapolis, MN, USA, pp. 1170-1175.

[5] D. Belega, D. Petri, "Performance of Synchrophasor Measurements Provided by the Weighted Least Squares Approach", Proc. 2013 Int. Instrum. Meas. Technol. Conf., I2MTC 2013, May 6-9, 2013, Minneapolis, MN, USA, pp. 946-951.

[6] M. Mishali, Y. C. Eldar, "Reduce and Boost: Recovering Arbitrary Sets of Jointly Sparse Vectors", *IEEE Trans. Signal Process.*, vol. 56, no. 10, pp. 4692-4702, Oct. 2008.